Journal of Alloys and Compounds 504S (2010) S14–S17

Contents lists available at ScienceDirect

Journal of Alloys and Compounds

journal homepage: www.elsevier.com/locate/jallcom

Glass formation in the Nb–Si binary system

K. Georgarakis[a,b,*], Y. Li[b], M. Aljerf[b], D. Dudina[b], A. LeMoulec[b], A.R. Yavari[b,a], G. Vaughan[c], A. Inoue[a]

[a] WPI-Advanced Institute for Materials Research, Tohoku University, Aoba-Ku, Sendai 980-8577, Japan
[b] Euronano SIMaP-CNRS, Institut National Polytechnique de Grenoble, 38402, St-Martin-d'Hères, France
[c] European Synchrotron Radiation Facility, 6 rue Jules Horowitz, 38042, Grenoble, France

ARTICLE INFO

Article history:
Received 5 July 2009
Received in revised form 26 February 2010
Accepted 2 March 2010
Available online 9 March 2010

Keywords:
Metallic glasses
Amorphous materials
Rapid quenching
Metals and alloys
X-ray diffraction
Crystallization

ABSTRACT

$Nb_{81.3}Si_{18.7}$ ribbons were prepared by rapid quenching of the liquid on a rotating copper wheel using various values of rotating speed. It was found that the melt spun ribbons consisted of an amorphous matrix; however the critical cooling rate for the formation of fully amorphous ribbons was achieved at rather high values of wheel speed. Crystallization occurs upon annealing above 971 K. The Vickers hardness of the amorphous ribbons was found to be 915 HV, an unusually high value for a binary alloy. The atomic structure of the amorphous Nb–Si alloy was studied using real space pair distribution (PDF)/radial distribution functions (RDF) derived from high precision X-ray diffraction data acquired with high-energy, monochromatic synchrotron light in transmission.

1. Introduction

Since the discovery of the first glassy alloy in 1960 [1], the field of metallic glasses has been extensively developed. A large number of alloys have been quenched to a glassy state, and a great increase of the maximum thickness of glassy metallic specimens from less than 100 μm to nearly 10 cm has been achieved, associated with a strong decrease in the critical cooling rate from 10^6 K/s to 1 K/s for the suppression of crystallization in the liquid state. This progress has come along with the better understanding of the criteria for easy glass formation [2–6]. The above achievements together with the enhanced properties of metallic glasses, such as high mechanical strength and large elastic deformation, good corrosion and wear resistance and good soft magnetic properties have led to several applications including sensors, parts for sport products and various springs, ornaments, micro-mirror and micro-tools, medical implants and more [7–10]. In addition, recent investigations on the atomistic level, using state of the art characterization tools such as synchrotron radiation and simulations have improved our understanding of the atomic structure and its correlation with the properties of metallic glasses [11–16].

A considerable amount of research efforts has been focused on refractory materials (RM) such as Nb–Si based alloys mainly because of their high melting temperatures, high oxidation resistance and good mechanical properties [17–19]. In addition, Nb–Si binary alloy system has attracted the attention of several investigators because of the possibility to form the metastable Nb_3Si intermetallic compound with A15 (cubic) structure which has high superconducting transition temperature in the range of 19–27 K [20,21]. Being metastable and thus not appearing in the equilibrium Nb–Si phase diagram, A15-Nb_3Si does not form with conventional methods for materials preparation. Furthermore, Nb_3Si may also form a body centred tetragonal structure which appears to be stable at temperatures higher than 1770 °C (Fig. 1) [22]. On the other hand, A15-Nb_3Si phase can be synthesized by devitrification of amorphous Nb–Si alloys upon annealing under high pressure [23,24]. Amorphous Nb–Si alloys can be prepared in the form of thin films (~100 nm) by sputtering deposition [25] and pulsed laser quenching at high cooling rates in the order of 10^{12} K/s [26], as well as in the form of foils and ribbons by rapid quenching via splat cooling and melt spinning, respectively [27,28]. However, some reports suggested the coexistence of amorphous and crystalline phases in ribbon specimens prepared by melt sinning [29,30]. In the present work, we report on the glass forming ability of the $Nb_{81.3}Si_{18.7}$ eutectic alloy by rapid quenching (melt spinning) and the crystallization behavior of the amorphous ribbons upon annealing.

2. Experimental procedures

$Nb_{81.3}Si_{18.7}$ master ingots (nominal composition) were carefully prepared by arc melting the pure elements in an argon inert atmosphere. The ingots were remelted at least five times in order to ensure homogeneity. Ribbons were produced from

* Corresponding author at: Euronano-INP Grenoble, 1130 rue de la Piscine, 38402, St-Martin-d'Hères, France. Tel.: +33 476826641; fax: +33 476826641.
E-mail addresses: georgara@minatec.inpg.fr, georgarakis@gmail.com (K. Georgarakis).

0925-8388/$ – see front matter © 2010 Elsevier B.V. All rights reserved.
doi:10.1016/j.jallcom.2010.03.034

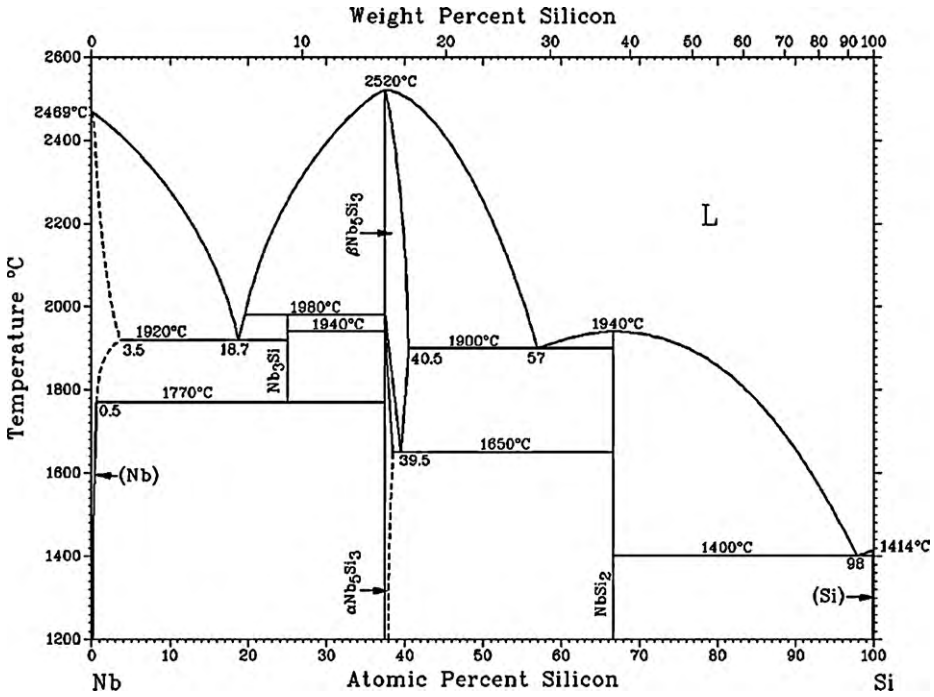

Fig. 1. Thermodynamic equilibrium phase diagram of the binary Nb–Si system [22].

the master ingots by rapid quenching of the liquid using the single roller melt spinning technique operating under helium atmosphere. The linear velocity of the rotating copper wheel was in the range of 43–64 ms^{-1}. Examination of the produced ribbons by electron dispersive spectroscopy (E.D.S.) established that they contained 82.3 ± 1.5 at.% Nb and 18.7 ± 1.5 at.% Si. Differential scanning calorimetry (DSC) was employed to study the thermal stability of the produced ribbons using a SETARAM HF-DSC device at a constant heating rate of 0.083 K/s. Ribbon samples were encapsulated under vacuum in quartz tubes and consequently annealed at various temperatures in the range of 873 K and 1373 K for 10 min. The annealing took place in a Heraeus laboratory oven, whereas the encapsulated samples were left to cool down to room temperature in air. The structure of as cast and annealed samples was studied by X-ray diffraction (XRD) using a Panalytical X'Pert Pro diffractometer with Cu K_α radiation. The microhardness was measured using a Buhler Micromet device equipped with a Vickers type indenter by applying a load of 50 g for 10 s.

The atomic structure of the amorphous Nb–Si binary alloys was investigated using real space pair distribution functions (PDF) derived from high precision synchrotron radiation X-ray diffraction data acquired in transmission mode at the ID11 of the European Synchrotron Radiation Facility (ESRF). The photon energy used was 70 keV corresponding to an X-ray wave-length of about 0.0177 nm. Further experimental details are given in Refs. [31,32].

3. Results and discussion

According to the equilibrium phase diagram of the Nb–Si binary system, Fig. 1, a deep eutectic appears in the Nb rich side at 18.7% Si with melting temperature at 2193 K (1920 °C) [22]. It is well known that most glass forming alloys are near eutectic compositions. Compared to the other compositions, the near eutectic liquids are stable at temperatures closest to the glass transition temperature [33,34]. Thus, the Nb–Si eutectic composition is expected to possess the highest possibility to form amorphous phase during quenching from the liquid state among the binary Nb–Si alloys.

Fig. 2 presents the XRD patterns from $Nb_{81.3}Si_{18.7}$ ribbons prepared by melt spinning at various values of linear velocity of the rotating copper wheel. The pattern corresponding to specimens prepared at the lowest used linear velocity (43 ms^{-1}) shows successive diffuse diffraction halos, characteristic of an amorphous phase. However, weak Bragg peaks are superimposed to the amorphous halos indicating the coexistence of crystalline phases within the amorphous matrix. Most of these peaks correspond to the A15-Nb_3Si metastable phase which has a cubic structure. In addition, the presence of a Nb_3Si phase with body centre tetragonal (bct) structure and a Nb_5Si_3-bct intermetallic phase cannot be excluded. With increasing the linear velocity of the rotating copper wheel up to 57 ms^{-1} and thus increasing the cooling rate, the Bragg peaks become even weaker, indicating a decrease of crystallinity in the melt spun samples. With further increase of the copper wheel velocity the Bragg peaks disappear entirely suggesting that the melt spun ribbons are fully amorphous and thus that the critical cooling rate for the formation of fully amorphous ribbons can be reached with wheel speed as high as 64 ms^{-1}. It is believed that the high cooling rates achieved at high wheel velocities suppress long range atomic diffusion required for the nucleation and growth of the competing phases such as the Nb solid solution (equilibrium phase), Nb_5Si_3-bct (equilibrium phase), Nb_3Si-bct (stable above 2043 K) and the metastable A15-Nb_3Si-cubic, all of which form at compositions far from the eutectic, thus favouring the formation of the amorphous phase [27]. However, the above observations indicate that the ability of the eutectic $Nb_{81.3}Si_{18.7}$ alloy to form a glass is sensible to the cooling rate and that the critical cooling rate for

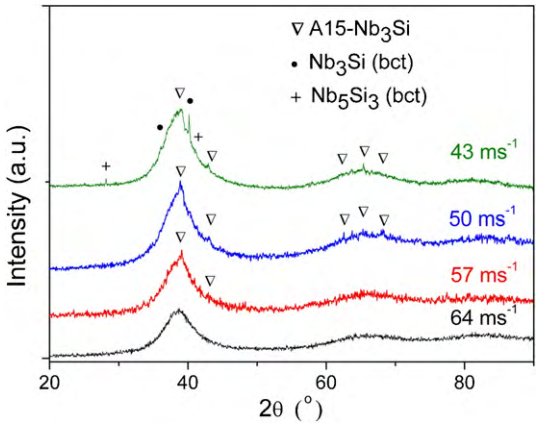

Fig. 2. X-ray diffraction patterns of melt spun Nb–Si ribbons prepared using different values of wheel linear velocity in the range of 43–64 ms^{-1}.

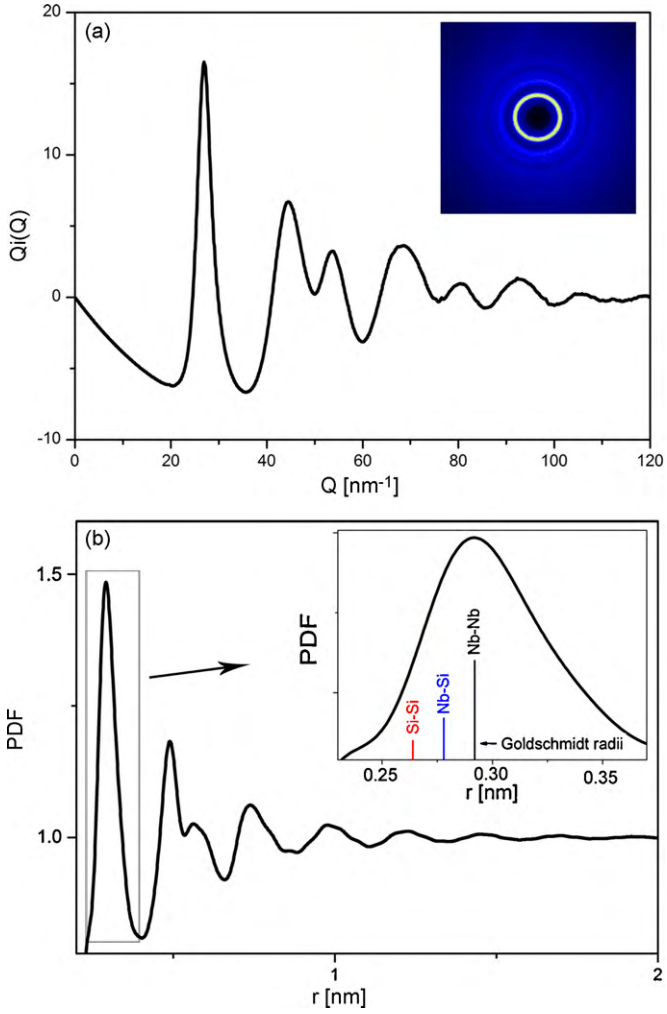

Fig. 3. (Inset a) X-ray diffraction 2D-pattern of an amorphous Nb–Si alloy, (a) the corresponding interference function Qi(Q), (b) the calculated pair distribution function PDF(r) and (inset b) a close-up of the first PDF peak.

preparing fully amorphous samples is rather high. Therefore this system can be characterized as a marginal glass former, in agreement with previous studies [30]. The glass forming ability of Nb–Si alloys has been shown to depend strongly not only on the cooling rate but also on the purity of the alloy and the starting elements [35].

The X-ray diffraction 2D-pattern of an amorphous Nb–Si alloy acquired using synchrotron radiation in transmission is shown in the inset of Fig. 3a, while the corresponding interference function Qi(Q) calculated from the XRD intensity profile after the necessary corrections is shown in Fig. 3a. The pair distribution function PDF(r) obtained by Fourier transformation is shown in Fig. 3b. A detectable medium-range order maintains until about 2 nm of the interatomic distance. A close-up of the first PDF peak is shown in the inset of Fig. 3b; the positions corresponding to the interatomic distances obtained using Goldschmidt atomic are also depicted. As expected, first PDF peak is dominated by the contribution of Nb–Nb atomic pairs.

Fig. 4 shows the DSC curve of a $Nb_{81.3}Si_{18.7}$ amorphous ribbon. An exothermic peak with onset at $T_x = 971$ K is observed, corresponding to the crystallization reaction of the amorphous phase. A second smaller in intensity and relatively wide exothermic peak appears on the right shoulder of the crystallization peak at 1043 K. It is believed that this is associated with grain growth phenomena of the formed crystals, since no dramatic difference can be observed

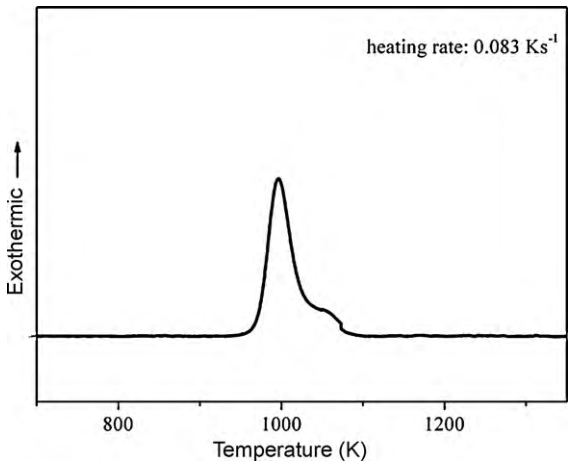

Fig. 4. DSC trace of $Nb_{81.3}Si_{18.7}$ amorphous ribbons.

between XRD patterns obtained after annealing at lower (1013 K) and higher (1123 K) temperatures than the temperature of this peak (Fig. 5).

The reduced glass transition temperature ($T_{rg} = T_g/T_m$), which is often used as one of the parameters associated with the glass forming ability, is about 0.44, while good glass forming alloys exhibit typically T_g/T_m values of 0.5–0.6 [2]. The rather low value of reduced glass transition temperature (T_{rg}) implied by a low value of T_g/T_m is another indication of the difficulty of the Nb–Si alloy to form amorphous phase.

X-ray diffraction patterns of $Nb_{81.3}Si_{18.7}$ ribbons after annealing for 10 min at different temperatures are presented in Fig. 5. The XRD curve of a ribbon annealed at 873 K indicates that the amorphous phase is preserved during heating up to this temperature, in agreement with the DSC results in Fig. 4. Upon heating to a higher temperature (1013 K), the amorphous phase crystallizes into a body centred tetragonal (bct) Nb_3Si phase and a body centred cubic (bcc) Nb solid solution. With further annealing to higher temperatures up to 1373 K the intensities of the Bragg peaks become higher and their full widths at half maximum (FWHM) become smaller indicating grain coarsening of the formed crystals. However, no evidence of phase transformation in the temperature range of 1123–1373 K can be observed from the XRD spectra (Fig. 5), in agreement with the DSC observations. The above results indicate that the metastable A15-Nb_3Si-cubic phase does not form upon annealing of the amorphous $Nb_{81.3}Si_{18.7}$ phase under the conditions used in this study. This finding is in agreement with older reports [23,24] claiming the

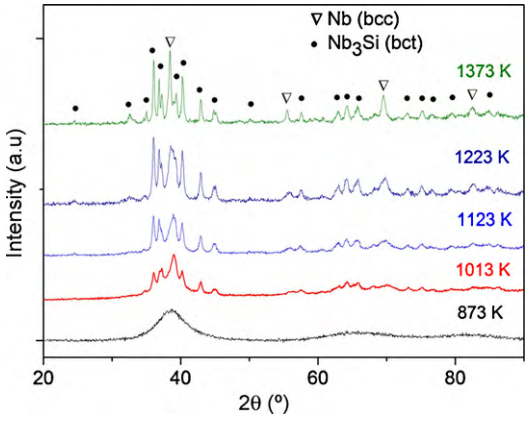

Fig. 5. X-ray diffraction patterns of melt spun $Nb_{81.3}Si_{18.7}$ ribbons after annealing for 10 min at various temperatures.

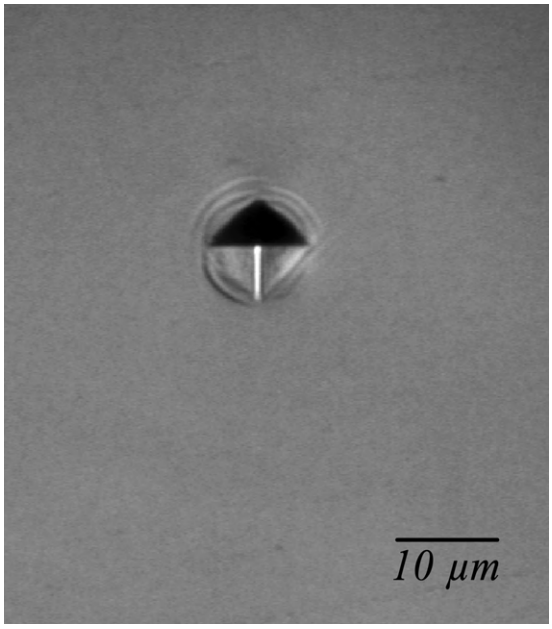

Fig. 6. Optical micrograph of a Vickers indentation track on $Nb_{81.3}Si_{18.7}$ amorphous ribbons.

need of application of high pressure of the order of 10 GPa during annealing of the amorphous Nb–Si in order to favour the formation of this interesting metastable phase. In addition, the results shown in Fig. 2 indicate the formation of small quantity of this metastable phase during rapid quenching and imply that lowering the cooling rate upon solidification may favour the formation of A15-Nb_3Si on the expense of the amorphous Nb–Si phase.

The microhardness of the melt spun amorphous ribbons, measured using a Vickers-type indenter, was found to be around 915 HV. This high value of microhardness is among the highest ever reported for a binary amorphous alloy. Using the well known relation $HV \approx 3\sigma_y$ which connects the hardness (HV) with the yield stress (σ_y) of metallic materials [36,37] the above mentioned hardness leads to a yield stress (σ_y) higher than 3 GPa. Compared to the compressive yield stress of about 1 GPa which was reported for a crystalline alloy with similar composition ($Nb_{82}Si_{18}$) [38], the mechanical strength of the amorphous phase is about three times higher. Observing the optical micrograph of a Vickers indentation of Fig. 6, clear evidence of the formation of shear bands with no cracking can be seen in the vicinity of the indentation track, indicating that the Nb–Si binary amorphous ribbons may exhibit some plasticity.

4. Conclusions

The glass forming ability and the crystallization upon annealing of the $Nb_{81.3}Si_{18.7}$ eutectic composition was investigated. It was found that high linear velocity of the wheel was needed to form fully amorphous ribbons by melt spinning and thus the ability of this alloy to form glass can be characterized as marginal. Upon annealing, the amorphous phase crystallizes above 971 K to a bct-Nb_3Si intermetallic phase and a bcc-Nb solid solution. The melt spun amorphous ribbons possess very high microhardness.

Acknowledgements

This work was funded by the French National Project (ANR-BLAN-036 VMM Ductiles) coordinated by A.R.Y., the World Premier Institute (WPI) of Tohoku University and the ESRF in the framework of a long-term project on metallic glasses.

References

[1] W. Klement, R.H. Willens, P. Duwez, Nature 187 (1960) 869.
[2] A. Inoue, Acta Mater. 48 (2000) 279.
[3] A.R. Yavari, A. Inoue, Mater. Res. Soc. Symp. Proc. 554 (1999) 21.
[4] A.L. Greer, Science 267 (1995) 1947.
[5] A.R. Yavari, J.L. Uriarte, A. Inoue, Mater. Sci. Forum 269–272 (1998) 533.
[6] A.R. Yavari, Phys. Lett. A 95 (1983) 165–168.
[7] W.L. Johnson, MRS Bull. 24 (1999) 42.
[8] A. Inoue, N. Nishiyama, MRS Bull. 32 (2007) 651.
[9] A.R. Yavari, J.J. Lewandowski, J. Eckert, MRS Bull. 32 (2007) 635.
[10] K. Georgarakis, M. Aljerf, Y. Li, A. LeMoulec, F. Charlot, A.R. Yavari, et al., Appl. Phys. Lett. 93 (2008), 031907.
[11] D.B. Miracle, Nat. Mater. 3 (2004) 697.
[12] H.W. Sheng, W.K. Luo, F.M. Alamgir, J.M. Bai, E. Ma, Nature 439 (2006) 419.
[13] A.R. Yavari, Nat. Mater. 4 (2005) 2.
[14] K. Georgarakis, A.R. Yavari, D.V. Louzguine, J. Antonowicz, M. Stoica, Y. Li, M. Satta, A. LeMoulec, G. Vaughan, Appl. Phys. Lett. 94 (2009) 191912.
[15] D.V. Louzguine-Luzgin, J. Antonowicz, K. Georgarakis, G. Vaughan, A.R. Yavari, A. Inoue, J. Alloys Compd. 466 (2008) 106.
[16] J. Antonowicz, D.V. Louzguine-Luzgin, A.R. Yavari, K. Georgarakis, M. Stoica, G. Vaughan, E. Matsubara, A. Inoue, J. Alloys Compd. 471 (2009) 70.
[17] J.H. Schneibel, M.J. Kramer, D.S. Easton, Scripta Mater. 46 (2002) 217–221.
[18] J. Geng, P. Tsakiropoulos, G. Shao, Mater. Sci. Eng. A 441 (2006) 26.
[19] M.N.R.V. Perdigao, J.A.R. Jordao, C.S. Kiminami, W.J.F. Botta, J. Non-Cryst. Solids 219 (1997) 170.
[20] D. Dew-Hughes, Cryogenics 15 (1975) 435.
[21] W.K. Wang, Y.Y. Wang, S.A. He, H. Iwasaki, Z. Phys. B: Condens. Matter 69 (1988) 481.
[22] T.B. Massalski, Binary Alloy Phase Diagrams, ASM, Materials Park, OH, 1986.
[23] C. Suryanarayana, W.K. Wang, H. Iwasaki, T. Masumoto, Solid State Commun. 34 (1980) 861.
[24] Y. Wang, W.K. Wang, S. Shouan, X.M. Huang, Chin. Phys. 10 (1990) 192.
[25] H. Iwasaki, W.K. Wang, N. Toyota, T. Fukase, H. Fulimori, Solid State Commun. 42 (1982) 381.
[26] F. Spaepen, in: E.W. Collings, C.C. Koch (Eds.), Proceedings of the Hume-Rothery Memorial Symposium, TMS-AINE, New Orleans, 1986, p. 187.
[27] R.M. Warerstrat, F. Haenssler, J. Muller, J. Appl. Phys. 50 (1979) 4763–4766.
[28] T. Masumoto, A. Inoue, S. Sakai, H. Kimura, A. Hoshi, Trans. Jpn. Inst. Met. 21 (1980) 115.
[29] G.A. Bertero, W.H. Hofmeister, M.B. Robinson, R.J. Bayuzick, Metall. Trans. A 22 (1991) 2713.
[30] L. Benderesky, F.S. Biancaniello, W.J. Boettinger, J.H. Perepezko, Mater. Sci. Eng. 89 (1987) 151.
[31] D.V. Louzguine-Luzgin, K. Georgarakis, G. Vaughan, A.R. Yavari, G. Xie, A. Inoue, J. Mater. Res. 20 (2009) 274.
[32] A.R. Yavari, A. Le Moulec, A. Inoue, J. Walter, F. Botta, G. Vaughan, A. Kvick, Mater. Sci. Eng. A 304–306 (2001) 34.
[33] M.H. Cohen, D. Turnbull, Nature 189 (1961) 131–132.
[34] A.R. Yavari, Nature 439 (2006) 405.
[35] K. Togano, H. Kumakura, K. Tachikawa, Phys. Lett. 76A (1980) 83.
[36] T.H. Courtney, Mechanical Behavior of Materials, 2nd ed., McGraw-Hill, Boston, 2000, p. 26.
[37] A.R. Yavari, K. Ota, K. Georgarakis, A. LeMoulec, F. Charlot, G. Vaughan, A.L. Greer, A. Inoue, Acta Mater. 56 (2008) 1830.
[38] Z. Li, L.M. Peng, Acta Mater. 55 (2007) 6573.